Proceedings of the ASME 2024 19th International Manufacturing Science and Engineering Conference MSEC2024
June 17 – June 21, 2024, Knoxville, Tennessee

MSEC2024-131699

BRIEF PAPER: A PRELIMINARY STUDY ON THE DYNAMICS OF MODULATED TURNING (MT) WITH SPINDLE SPEED VARIATION (SSV)

Mert Ozdemir
Oregon State University
Corvallis, OR

Burak Sencer
Oregon State University
Corvallis, OR

ABSTRACT

This paper proposes a novel strategy to enhance dynamic stability of turning processes. It presents a novel assistive strategy, which combines Spindle Speed Variation (SSV) and Sinusoidal Tool Modulations to dramatically improve chatter stability of high-speed turning. Chatter vibrations are a type of self-exiting vibrations that originate due to the dynamic flexibilities in the machine/workpiece/tool. Once chatter is triggered, it rapidly grows to destroy the surface finish, harms the tool and even the machine tool components. Chatter is the most limiting factor restricting productivity and attenable material removal rates (MRR) in most high-speed turning operations. A well-known strategy to improve chatter stability in turning is to use SSV. Continuously varying the spindle speed helps disturb and weaken the regenerative effect (regenerations) and thus improve chatter stability. Most recently, it is also reported that adding sinusoidal tool modulations also help improve chatter stability. This process is called the modulated turning (MT), and sinusoidal tool modulations cause the tool to disengage from the workpiece (cut) repeatedly introducing time for the regeneration effect to die out. This paper, for the first time, proposes to utilize sinusoidal tool modulations and SSV at the same time to assist and improve chatter stability of turning even further. The semi-discrete time domain approach is utilized to analyze chatter stability of this newly created turning process. It is observed, that jointly using tool modulations and SSV provides greater asymptotic chatter stability margins enabling average 10~20% greater material removal rates to be achieved. Furthermore, it modifies existing stability lobes and helps create additional lobes, which may be utilized to maximize material removal rate at other desired target spindle speeds. Overall, joint application of SSV and tool modulations provide greater stability in turning.

Keywords: machining dynamics, chatter, turning

1. INTRODUCTION

Turning is one of the oldest and most widely used machining processes. However, it suffers greatly from regenerative chatter vibrations especially at high cutting speeds [1]. There have been various strategies to help mitigate chatter vibrations in turning such as processing planning using chatter stability lobe diagrams (SLDs) [2], utilizing tools with passive and active dampening mechanisms [3], utilizing support for flexible workpieces [4] to name a few. SLD provide stable cutting conditions but do not dampen chatter to increase productivity. Assistive strategies capital intensive, require added hardware and thus have limited use.

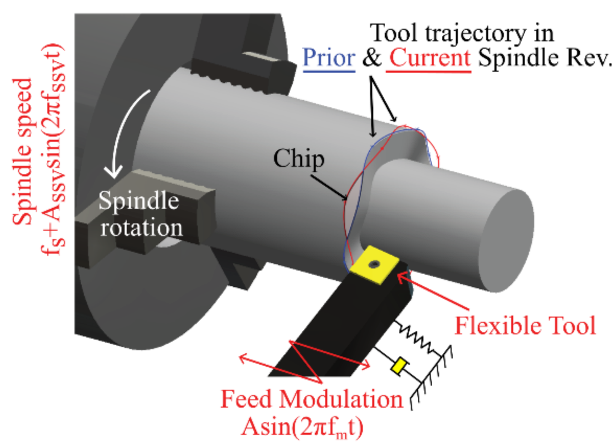

FIGURE 1: SSV+MT process kinematics

Spindle speed variation (SSV) has been a well-known assistive strategy to improve chatter stability in turning and even offered in most automated lathes as a commercial functionality [5] to the end-user. SSV modulates the spindle speed sinusoidally and slowly around the set speed to disturb the regeneration effect, and hence improve chatter stability. Although it is effective, its advantage is limited since it is most effective at low-speed region where the use of process damping [6] is already favored, and to attain greater stability at high speed, SSV requires high-frequency and high-amplitude modulations that cannot be realized due to power/torque rating of the machine tool's drives [7].

Modulated turning (MT) has been also proposed as a novel assistive strategy for turning [8]. But. its main advantage was considered facilitating robust chip breaking. As compared to SSV, MT modulates the tool in the feed direction rather than the spindle, and it converts continuous turning process into discrete cutting. It has been also reported that MT also helps improve chatter stability of turning [9].

This paper proposes and investigates the dynamics of joint application of SSV and MT (SSV+MT) for high-performance turning. The idea is to utilize both the SSV and the MT at the same time (See Fig. 1) to further improve the chatter stability. The following sections model kinematics of the process and provide an analytical stability analysis using the semi-discrete method[7].

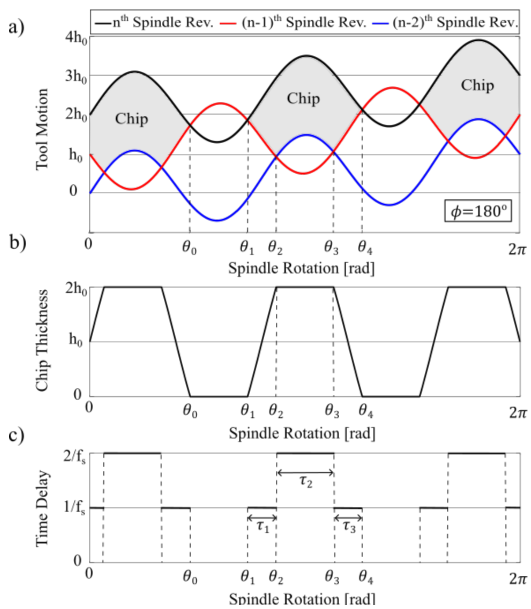

FIGURE 2: Tool trajectory, chip formation and time delay for $\phi = \pi$

2. DYNAMICS OF SSV+MT ASSISTED TURNING

2.1. Modulated turning (MT) process kinematics and delay formation

In MT, the tool motion is sinusoidally modulated in the feed direction [8] around a nominal feedrate h_0 as shown in Fig. 1.

$$y(t) = h_0 f_s t + A \sin(2\pi f_m t) \tag{1}$$

where f_s is the spindle rotation frequency and f_m is the tool modulation frequency. Equation (1) can be written with respect to spindle angle θ and (spindle) revolution counter n as:

$$y_n(\theta) = (n-1)h_0 + \frac{h_0\theta}{2\pi} A \sin\left(\frac{\theta f_m}{f_s} + (n-1)\phi\right) \tag{2}$$

where $\phi = 2\pi(f_m/f_s - int[f_m/f_s])$ indicates the phase shift of tool modulations, undulations left on the work surface, between successive spindle revolutions [8]. When the modulation amplitude $A > h_0/2 \sin\left(\frac{\phi}{2}\right)$, tool disengages from the workpiece enabling discrete cutting with an uncut chip thickness variation illustrated in Fig. 2. In this example $\phi = \pi$ is used, and as shown in Fig. 2b, the uncut chip thickness has 3 parts. At the beginning, the chip is formed between the current tool motion and previously left surface. In the middle section, the chip is cut from the work surface left two revolutions before, and at the last section of the chip is generated from the work surface cut in the previous revolution. As shown in Fig.2b, chip formation is periodic with the modulation frequency, and spindle's angular positions $\theta_1, \theta_2, \theta_3, \theta_4$ represent borders of chip sections as [10]:

$$\theta_1 = \frac{f_s}{f_m}\left(\pi - \sin^{-1}\frac{h_0}{2A}\right) \quad \theta_2 = \frac{f_s}{f_m}\left(\pi + \sin^{-1}\frac{h_0}{2A}\right)$$
$$\theta_3 = \frac{f_s}{f_m}\left(2\pi - \sin^{-1}\frac{h_0}{2A}\right) \quad \theta_4 = \frac{f_s}{f_m}\left(2\pi + \sin^{-1}\frac{h_0}{2A}\right) \tag{3}$$

It should be noted that in regenerative chatter stability, delays in generating dynamic cutting forces play the key role [11]. As shown in Fig. 2c the MT process exhibits multiple delays (regenerations) since the chip is formed through multiple spindle revolutions. Duration of the delays depends on the length of chip sections and Eq. (3) indicates that it is controlled by the spindle frequency f_s. Intersection of tool trajectories in successive spindle revolutions can be used to compute the delay from Eq. (2) as:

$$\tau = \begin{cases} \tau_1, & \theta_1 < mod(\theta, 2\pi) \leq \theta_2 \\ \tau_2, & \theta_2 < mod(\theta, 2\pi) \leq \theta_3 \\ \tau_3, & \theta_3 < mod(\theta, 2\pi) \leq \theta_4 \end{cases} \tag{4}$$

and it is depicted in Fig. 2c. For $\phi = \pi$, the delay sequence is rather simple where delay alters between 1 and 2 spindle revolutions. In general form, delay sequence vary depending on the f_m/f_s ratio and A, and detailed in the literature [11]. This paper focuses on the condition when $\phi = \pi$, which is the most widely used MT condition in practice [8].

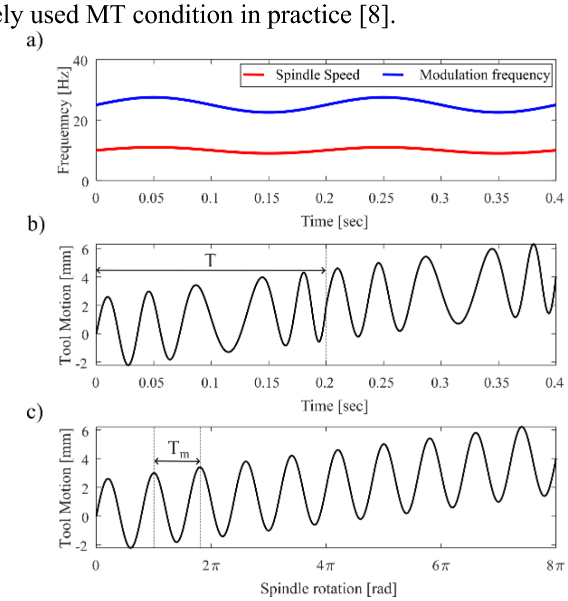

FIGURE 3: (a) Variation of spindle speed and modulation frequency; (b) Tool motion in time domain; (c) Tool motion with respect to angular position of the workpiece

2.2. Kinematics and delay formation of modulated turning with spindle speed variation (MT+SSV)

When SSV is applied, spindle speed (f_s) is also modulated sinusoidally around a nominal value as:

$$f_s(t) = f_{s0} + A_{SSV} \sin(2\pi f_{SSV} t) \tag{5}$$

with $RVA = A_{SSV}/f_{s0}$ and $RVF = f_{SSV}/f_{s0}$ denoting the magnitude and frequency ratio of the spindle speed modulations. In this case, the time delay between present and previous cuts for conventional turning operation is as follows [7].

$$\int_{t-\tau(t)}^{t} f_s(\sigma) d\sigma = 1 \tag{6}$$

It should be noted that when SSV is applied during MT at a constant f_{SSV}, phase angle ϕ (phase between waves on undulated work surface) varies, which disrupts periodic chip formation. Hence, the tool modulation frequency f_m must be altered synchronously with the spindle speed f_s to maintain a constant phase angle. The change of spindle speed and tool modulation frequency are presented in Fig. 3a. The tool motion in time domain is shown in Fig. 3b. The tool motion in time domain does not exhibit behavior of a normal sinusoidal function due to changes in modulation frequency over time. However, tool motion with respect to angular position of the workpiece follows a basic sinusoidal function as shown in Fig. 3c. This is because the relation between modulation frequency and spindle speed is linear. The period of tool modulations in angular domain T_m is expressed as:

$$T_m = 2\pi/(f_m/f_s) \tag{7}$$

Here, it should be noted that the time periodicity of the tool motion becomes $T = 1/(f_{s0}RVF)$, which also serves as the principal period of the system [7]. The relationship between spindle rotation and spindle speed can be written as:

$$\theta(t) = \int_0^t 2\pi f_s(\sigma) d\sigma \tag{8}$$

Figure 4 presents the chip thickness variation in time domain with SSV. The duration material removal for each individual discrete chip segment changes due to varying spindle speed. The time stamps that determine the starting and ending point of each chip segment can be derived using Eqs. (3) and (8) as:

$$\begin{aligned} &\int_0^{t_{k,1}} 2\pi f_s(\sigma) d\sigma = \theta_1 + kT_m, \\ &\int_0^{t_{k,2}} 2\pi f_s(\sigma) d\sigma = \theta_2 + kT_m \\ &\int_0^{t_{k,3}} 2\pi f_s(\sigma) d\sigma = \theta_3 + kT_m \\ &\int_0^{t_{k,4}} 2\pi f_s(\sigma) d\sigma = \theta_4 + kT_m \end{aligned} \tag{9}$$

where k represents number of the discrete chip within one principal period *T*. $t_{k,1}, t_{k,2}, t_{k,3}$ and $t_{k,4}$ denote the sections of the k^{th} chip formation in time domain within one principal period, and the integral terms from Eq. (9) are derived algebraically as:

$$\begin{aligned} &2\pi f_{s0} t_{k,1} + \frac{RVA}{RVF}\left[1 - cos\left(2\pi RVF f_{s0} t_{k,1}\right)\right] \\ &\qquad = \theta_1 + kT_m \\ &2\pi f_{s0} t_{k,2} + \frac{RVA}{RVF}\left[1 - cos\left(2\pi RVF f_{s0} t_{k,2}\right)\right] \\ &\qquad = \theta_2 + kT_m \\ &2\pi f_{s0} t_{k,3} + \frac{RVA}{RVF}\left[1 - cos\left(2\pi RVF f_{s0} t_{k,3}\right)\right] \\ &\qquad = \theta_3 + kT_m \\ &2\pi f_{s0} t_{k,4} + \frac{RVA}{RVF}\left[1 - cos\left(2\pi RVF f_{s0} t_{k,4}\right)\right] \\ &\qquad = \theta_4 + kT_m \end{aligned} \tag{10}$$

Time stamps $t_{k,1}, t_{k,2}, t_{k,3}$ and $t_{k,4}$ are then solved from Eq.(10) by using root finding algorithms such as secant method.

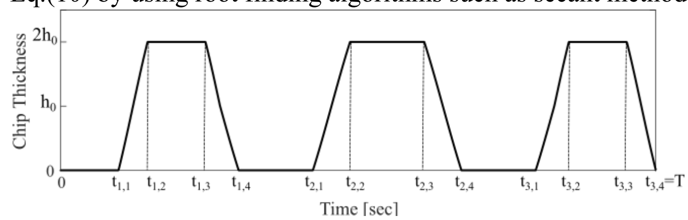

FIGURE 4: Chip formation in MT+SSV process; $\phi = 180°, A/h_0 = 1$, $f_m/f_s = 1.5$. $RVA = 0.1$, $RVF = 0.5$

As noted, SSV modulates chip formation in time domain causing delays to become time varying as well. As a result, the SSV+MMT process becomes a time-varying multi-delay system. For $\phi = 180°$, the time delay function is expressed by using Eq.(6).

$$\tau(t) = \begin{cases} \int_{t-\tau_1(t)}^{t} f_s(\sigma) d\sigma = 1, & t_{k,1} \le t < t_{k,2} \\ \int_{t-\tau_2(t)}^{t} f_s(\sigma) d\sigma = 2, & t_{k,2} \le t < t_{k,3} \\ \int_{t-\tau_3(t)}^{t} f_s(\sigma) d\sigma = 1, & t_{k,3} \le t < t_{k,4} \end{cases} \tag{11}$$

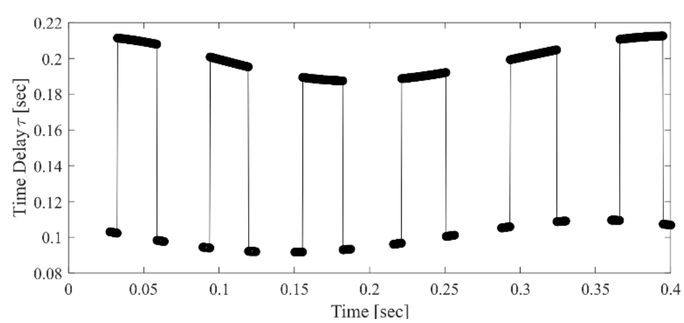

FIGURE 5: Time varying delay within principal period; $\phi = 180$, $A/h_0 = 2$, $f_m/f_s = 1.5$, $RVA = 0.1$, $RVF = 0.25$

The time delay $\tau(t)$ is a piecewise varying function (See Eq.(11). The delay represents the time required for the completion of one spindle revolution during the removal of the first segment of the chip. For the second segment, the time delay is equivalent to the time needed for two complete spindle revolutions. Lastly, for the third segment, the time delay equals the time required for one complete spindle revolution.

Time-varying delay in SSV+MT process has been illustrated by solving Eq.(11) over one principal period using the cutting conditions and depicted in Fig. 5. Note that the time-varying delay exhibits a sinusoidal behavior due to the application of SSV with oscillations centered around $1/f_{s0}$ and $2/f_{s0}$.

3. Chatter stability of SSV+MT assisted turning using the semi-discrete method

This section presents the stability analysis of the SSV+MT turning using the semi-discrete method [7]. Figure 1 illustrates the simplified dynamics of the process with a flexible tool. As shown, the tool is flexible only in the feed direction with a single mode, and equation of motion of the process can be written as:

$$\begin{aligned} \ddot{y}_d(t) + 2\zeta\dot{y}_d(t) + \omega_n^2 y_d(t) &= F_d(t) \\ &= \frac{\omega_n^2}{k_y} K_f b\big[-g_{cut}(t)y_d(t) \\ &\quad + g_{cut}(t)y_d\big(t-\tau(t)\big)\big] \end{aligned} \tag{12}$$

$$\begin{cases} g_{cut}(t) = 1, & t_{k,1} < t < t_{k,4} \\ g_{cut}(t) = 0, & otherwise \end{cases}$$

where ω_n *and* ζ denote the modal parameters, K_f [MPa] is the (feed) cutting force coefficient, b [m] is the cutting width, k_y is the stiffness in feed direction, $\tau(t)$ is the time varying delay and $g_{cut}(t)$ is the windowing function, which indicates when the tool is in-cut, $g_{cut}(t) = 1$, for $t_{k,1} < t < t_{k,4}$.

Equation of motion from Eq.(12) can be re-written in state space form as:

$$x_1 = y_d(t)$$
$$x_2 = \dot{y}_d(t)$$

$$\begin{Bmatrix} \dot{x}_1 \\ \dot{x}_2 \end{Bmatrix} = \begin{bmatrix} 0 & 1 \\ -\omega_2^2\left(1+\dfrac{g_{cut}(t)K_f a}{k_y}\right) & -2\zeta\omega_n \end{bmatrix} \begin{Bmatrix} x_1 \\ x_2 \end{Bmatrix} + \begin{bmatrix} 0 & 0 \\ \dfrac{\omega_n^2}{k_y}K_x b g_{cut}(t) & 0 \end{bmatrix} \begin{Bmatrix} x_1(t-\tau(t)) \\ 0 \end{Bmatrix} \tag{13}$$

and converted into discrete state-space representation as:

$$\dot{x}(t) = A_i x(t) + B_i x(t-\tau_i(t)), t \in [t_i, t_{i+1}) \tag{14}$$

where $t_i = i\Delta t$ is the discrete time with a discretization time step of Δt. The discretization time step is critical for the accuracy of the application of the semi-discrete stability analysis [7].

Δt is calculated using the principal period of the system T with a period resolution of p, yielding $\Delta t = T/p$. Note that the period resolution needs to be chosen to be sufficiently large to ensure the sensitivity of the model. $x(t-\tau_i)$ represents the delayed state with time-varying delay, and it is approximated by averaging two consecutive samples as:

$$x(t_i - \tau_i) = \frac{1}{2}\left(x_{i-r_i+1} + x_{i-r_i}\right) \tag{15}$$

where $r_i = int(\tau_i(t)/\Delta t)$ represents delay samples for the delayed states. The solution over one discrete step can be formulated as:

$$x_{i+1} = L_i x_i + \frac{1}{2}R_i(x_{i-r_i+1} + x_{i-r_i}) \tag{16}$$

where, $L_i = e^{A_i\Delta t}$, $R_i = (e^{A_i} - I)A_i^{-1}B_i$, and I denotes for 2×2 identity matrix. The discrete map becomes:

$$\begin{gathered} z_{i+1} = G_i z_i \\ z_i = [x_i, x_{i-1}, \dots, x_{i-r}]^T \end{gathered} \tag{17}$$

The augmented state transition matrix G_i is derived as:

$$\begin{array}{cc} & \begin{array}{cccccccccc} 1 & & & r_i & r_i+1 & & & & & r \\ \downarrow & & & \downarrow & \downarrow & & & & & \downarrow \end{array} \\ G_i = & \begin{bmatrix} L_i & 0 & \dots & 0 & \frac{1}{2}R_i & \frac{1}{2}R_i & 0 & \dots & 0 & 0 \\ I & 0 & \dots & 0 & 0 & 0 & 0 & \dots & 0 & 0 \\ 0 & I & \dots & 0 & 0 & 0 & 0 & \dots & 0 & 0 \\ \vdots & & & & & & & & 0 & \vdots \\ 0 & 0 & \dots & 0 & 0 & 0 & 0 & \dots & I & 0 \end{bmatrix} \end{array} \tag{18}$$

Here, $r = \max(r_i)$, $i = 1, 2, \dots, p$. The monodromy matrix Φ is obtained by p repeated applications of the discrete map, i.e., $\Phi = G_{p-1}G_{p-2}\dots G_0$.

According to the Floquet theory [7], the system's stability can be tested based on the eigenvalues of the monodromy matrix, $\lambda = eig(\Phi)$. If the absolute of any its eigenvalues exceeds unity, ($|\lambda| > 1$), the system is considered unstable, which indicates that the MT+SSV assisted turning process suffers from regenerative chatter vibrations.

4. RESULTS

The semi-discrete method is utilized to generate SLD for four different turning operations namely, SSV+MT, only MT, only SSV and for the conventional turning. The parameters used in simulations are provided in Table 1.

Parameter	Unit	Value
Cutting coefficient in feed direction K_y	N/mm^2	1338
Natural frequency of tool ω_n	rad/s	1570.8
Damping ratio ζ	-	0.0273
Stiffness in feed direction k_y	N/m	1.46×10^7
RVA	-	0.1
RFV	-	0.5
Ratio of modulation frequency and spindle rotating frequency f_m/f_s	-	2.5
Ratio of modulation amplitude to nominal feedrate A/h_0	-	3.0

Table 1: Parameters used in proposed chatter stability prediction

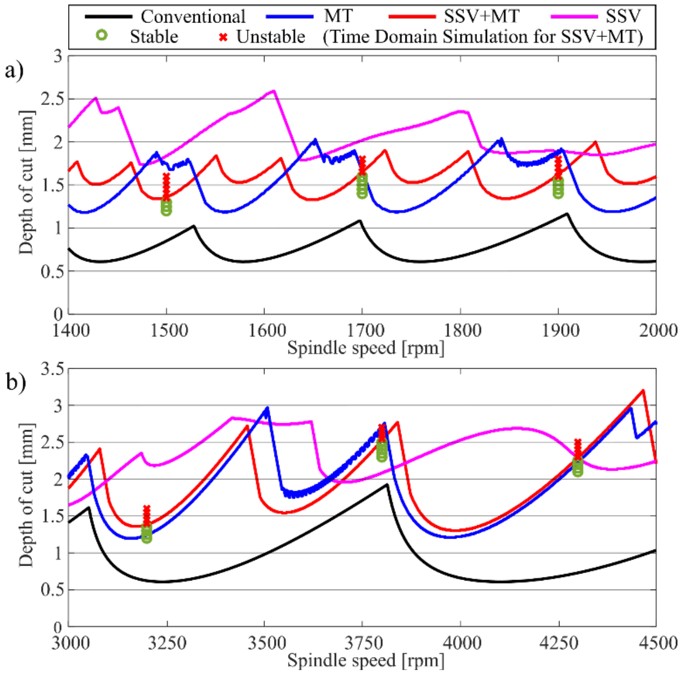

FIGURE 6: (a) Stability lobes diagrams for different turning processes in low-speed domain; (b) Stability lobes diagrams for different turning processes in high-speed domain

Figure 6a shows the chatter stability boundaries in low speed cutting region. Firstly, all the assisted turning processes exhibit better chatter stability than the conventional turning. The most effective method for achieving stable cutting with a high depth cut is with SSV. While both MT and SSV+MT also improve chatter stability compared to conventional turning, their difference is relatively small. When comparing MT and SSV+MT processes, it is observed that SSV+MT processes increases asymptotic stability by around 10% compared to MT.

Figure 6b shows the chatter stability boundaries for high-speed cutting region. As shown, only SSV remains to be a good choice for achieving highest stability. The impact of speed variation on chatter stability in SSV+MT becomes insignificant during high spindle speed operations, as deduced from a comparison of stability lobes between MT and SSV+MT.

The SSV+MT process is simulated in time domain to verify accuracy of semi-discrete method. The time domain simulation strategy presented by [11] is adapted with implementation of speed variation during material removal.

When the operation requires chip breaking, as is often the case in machining ductile materials, the use of MT is very effective. The results also indicate that adding SSV to the MT process can enhance stability. If the goal is to achieve high material removal rates without considering chip breaking, using only SSV becomes the most effective solution.

5. CONCLUSION

This paper presented preliminary study on the stability of SSV assisted modulated turning (MT). It showed that the stability can be analyzed using the semi-discrete method. Preliminary results show that using SSV and MT at the same time provides marginal improvement on the chatter stability of the process. However, the results are preliminary as various SSV and MT process conditions are not tested. Furthermore, the surface finish and robustness of the strategy must be investigated.

ACKNOWLEDGEMENTS

This research is supported by US's National Science Foundation (NSF Award no: 2019370).

REFERENCES

[1] Altintas, Y., 2012, *Manufacturing Automation: Metal Cutting Mechanics, Machine Tool Vibrations, and CNC Design*, Cambridge University Press.

[2] Altintas, Y., Stepan, G., Merdol, D., and Dombovari, Z., 2008, "Chatter Stability of Milling in Frequency and Discrete Time Domain," CIRP J Manuf Sci Technol, **1**(1), pp. 35–44.

[3] Munoa, J., Beudaert, X., Dombovari, Z., Altintas, Y., Budak, E., Brecher, C., and Stepan, G., 2016, "Chatter Suppression Techniques in Metal Cutting," CIRP Annals, **65**(2), pp. 785–808.

[4] Zeng, S., Wan, X., Li, W., Yin, Z., and Xiong, Y., 2012, "A Novel Approach to Fixture Design on Suppressing Machining Vibration of Flexible Workpiece," Int J Mach Tools Manuf, **58**, pp. 29–43.

[5] Insperger, T., and Stepan, G., 2004, "Stability Analysis of Turning With Periodic Spindle Speed Modulation Via Semidiscretization," Journal of Vibration and Control, **10**(12), pp. 1835–1855.

[6] Tuysuz, O., and Altintas, Y., 2019, "Analytical Modeling of Process Damping in Machining," Journal of Manufacturing Science and Engineering, Transactions of the ASME, **141**(6), pp. 1–16.

[7] Insperger, T., and Stépán, G., 2011, *Semi-Discretization for Time-Delay Systems: Stability and Engineering Applications*, Springer Science \& Business Media.

[8] Mann, J. B., Guo, Y., Saldana, C., Compton, W. D., and Chandrasekar, S., 2011, "Enhancing Material Removal Processes Using Modulation-Assisted Machining," Tribol Int, **44**(10), pp. 1225–1235.

[9] Eren, B., and Sencer, B., 2020, "Mechanistic Cutting Force Model and Specific Cutting Energy Prediction for Modulation Assisted Machining," Procedia Manuf, **48**, pp. 474–484.

[10] Nam, S., Eren, B., Hayasaka, T., Sencer, B., and Shamoto, E., 2021, "Analytical Prediction of Chatter Stability for Modulated Turning," Int J Mach Tools Manuf, **165**(November 2020), p. 103739.

[11] Eren, B., Nam, S., and Sencer, B., 2022, "Generalized Mechanics and Dynamics of Modulated Turning," J Mater Process Technol, **308**(July), p. 117708.